Small-molecule factor B inhibitor for the treatment of complement-mediated diseases

Anna Schubart[a,1], Karen Anderson[b,c,1], Nello Mainolfi[b,d], Holger Sellner[a], Takeru Ehara[b,e], Christopher M. Adams[b], Aengus Mac Sweeney[a,f], Sha-Mei Liao[b], Maura Crowley[b], Amanda Littlewood-Evans[a], Sophie Sarret[a], Grazyna Wieczorek[a], Ludovic Perrot[a], Valérie Dubost[a], Thierry Flandre[a], Yuzhou Zhang[g], Richard J. H. Smith[g], Antonio M. Risitano[h], Rajeshri G. Karki[b], Chun Zhang[b], Eric Valeur[a,i], Finton Sirockin[a], Bernd Gerhartz[a,j], Paulus Erbel[a], Nicola Hughes[a], Thomas M. Smith[b], Frederic Cumin[a], Upendra A. Argikar[b], Börje Haraldsson[a], Muneto Mogi[b], Richard Sedrani[a], Christian Wiesmann[a], Bruce Jaffee[b], Jürgen Maibaum[a], Stefanie Flohr[a], Richard Harrison[a,k], and Jörg Eder[a,2]

[a]Novartis Institutes for BioMedical Research, Novartis Pharma AG, CH-4056 Basel, Switzerland; [b]Novartis Institutes for BioMedical Research, Cambridge, MA 02139; [c]Ophthalmology, Biogen, Cambridge, MA 02142; [d]Kymera Therapeutics, Cambridge, MA 02139; [e]PeptiDream Inc., Kawasaki-shi, 210-0821 Kanagawa, Japan; [f]Drug Discovery Biology, Idorsia Pharmaceuticals Ltd., 4123 Allschwil, Switzerland; [g]Molecular Otolaryngology and Renal Research Laboratories, Carver College of Medicine, University of Iowa, Iowa City, IA 52242; [h]Department of Clinical Medicine and Surgery, Bone Marrow Transplantation Program, Federico II University, 80138 Naples, Italy; [i]Medicinal Chemistry, Cardiovascular, Renal & Metabolism, Innovative Medicines and Early Development Biotech Unit, AstraZeneca, 431 83 Mölndal, Sweden; [j]Protein Sciences, Abcam PLC, CB4 0GZ Cambridge, United Kingdom; and [k]Institute of Infection and Immunity, School of Medicine, Cardiff University, CF14 4XN Cardiff, United Kingdom

Dysregulation of the alternative complement pathway (AP) predisposes individuals to a number of diseases including paroxysmal nocturnal hemoglobinuria, atypical hemolytic uremic syndrome, and C3 glomerulopathy. Moreover, glomerular Ig deposits can lead to complement-driven nephropathies. Here we describe the discovery of a highly potent, reversible, and selective small-molecule inhibitor of factor B, a serine protease that drives the central amplification loop of the AP. Oral administration of the inhibitor prevents KRN-induced arthritis in mice and is effective upon prophylactic and therapeutic dosing in an experimental model of membranous nephropathy in rats. In addition, inhibition of factor B prevents complement activation in sera from C3 glomerulopathy patients and the hemolysis of human PNH erythrocytes. These data demonstrate the potential therapeutic value of using a factor B inhibitor for systemic treatment of complement-mediated diseases and provide a basis for its clinical development.

complement | alternative pathway | factor B | drug discovery | nephropathy

Complement is a key component of the innate immune system and an effective first-line defense against invading pathogens. It recognizes foreign cell surfaces and induces cell lysis/killing and inflammatory responses (1, 2). C3 is the central component of the system. Depending on the trigger, three distinct pathways (classical, lectin, and alternative), which converge at the proteolytic cleavage of C3 to generate C3a and C3b fragments, can initiate its activation. The major effector mechanisms elicited by the complement system are phagocytic elimination through C3-dependent opsonization, anaphylatoxin-mediated inflammatory cell recruitment, and cell lysis through generation of the membrane attack complex (MAC). The alternative pathway acts as an amplification loop of the other two pathways. Upon dysregulation, either due to inherited or acquired genetic mutations or to the presence of autoantibodies, alternative complement pathway (AP) activity can cause a number of diseases such as age-related macular degeneration (3), paroxysmal nocturnal hemoglobinuria (PNH) (4), atypical hemolytic uremic syndrome (5), and C3 glomerulopathy (C3G) (6). In addition, recent studies have revealed that the AP may also contribute to a number of Ig-mediated kidney pathologies, including IgA nephropathy and primary membranous nephropathy, where locally deposited immune complexes activate the complement cascade (7).

AP activation depends on the proteolytic cleavage of factor B (FB), a trypsin-like serine protease which circulates in human blood in a latent zymogen form at a concentration of about 3 μM

(8–11). During the central amplification step of the AP, C3b-bound FB is cleaved by factor D (FD) to generate C3bBb, the C3 convertase containing the FB catalytic subunit (Bb) (11). C3 convertase cleaves C3 to produce additional C3b, thereby further amplifying the local complement response. Binding of a second C3b molecule to the C3 convertase complex generates a C5 convertase complex, C3bBbC3b, thereby shifting substrate specificity from C3 to C5 and leading to MAC formation and C5a anaphylatoxin

Significance

Complement is a key component of the innate immune system; however, its dysregulation due to genetic mutations or the presence of autoantibodies can cause a number of diseases including age-related macular degeneration, paroxysmal nocturnal hemoglobinuria, and C3 glomerulopathy. The alternative pathway acts as an amplification loop of the complement system. It is triggered by the activation of factor B, the proteolytically active component of the C3 and C5 convertases. We report the discovery of a small-molecule inhibitor of factor B and demonstrate that it can efficiently block the alternative pathway in vivo in animals and ex vivo in patient samples. The compound is highly selective and potent and is currently in clinical development for a number of complement-mediated diseases.

generation. The active site of FB, either in its latent form or as part of the C3 and C5 convertase complexes, exists in an inactive conformation (12–14). Known covalent inhibitors of FB, including nafamostat and peptide aldehydes (15, 16), lack specificity, and to date no FB inhibitor is available for therapeutic application. The high abundance of latent FB presents an additional challenge for drug discovery as full blockade would require high systemic drug levels if the inhibitor cannot discriminate between active and latent FB forms.

Results and Discussion

To identify small-molecule FB inhibitors, we screened a chemically diverse subset (2.5×10^5 compounds) of our compound collection for direct inhibition of FB (*SI Appendix*, Table S1) using a proteolytic assay that employed a cobra venom factor (CVF):Bb complex as stable surrogate of the C3 convertase (*SI Appendix*, Fig. S1) (17). The screen identified the naphthalene-dihydro-imidazole amine compound **1** (Fig. 1*A*), which inhibits FB with a half-maximal inhibitory concentration (IC$_{50}$) of $6.6 \pm 3.5 \mu M$ ($n = 22$). The cocrystal structure of compound **1** bound to the catalytic domain of human FB at 1.64 Å resolution (Fig. 1*B* and *SI Appendix*, Table S2) shows the imidazoline ring to bind into the S3 pocket (18) in close contact to Pro172D (chymotrypsin numbering system) and forming a hydrogen bond between the imidazoline NH of compound **1** and the Gly216 carbonyl. The naphthyl ring builds a cation–π interaction to the guanidine group of Arg192.

In a first step, compound **1** was optimized for better drug-like properties. The naphthyl was replaced by an indole ring that fills the S1 pocket more efficiently. The indole NH forms a hydrogen bond with the Thr190 side chain, and its 7-methyl moiety expands toward the bottom of the pocket. The dihydro-imidazole amine was replaced by a piperidine, which conserves the hydrogen bond interaction to Gly216 but shifts Pro172D outward by 2.8 Å (compound **2**; Fig. 1 *A* and *C*). The crystal structure of FB with compound **2** also revealed a sulfate ion to be bound in close proximity to the piperidine ring and having multiple interactions with the protein (Fig. 1*D*). To further increase the potency of compound **2**, we made use of this interaction network by introducing a benzoic acid moiety in position 2 of the piperidine ring, which forms hydrogen bonds to both the Asn220B side chain and the Asp218A-NH. Replacement of the methoxy by an ethoxy group and substitution of the 5-methyl by a methoxy group on the indole ring led to LNP023, a highly potent FB inhibitor (Fig. 1 *A* and *D*). LNP023 showed direct, reversible, and high-affinity binding to human FB as determined by surface plasmon resonance (SPR) (K_D value of $0.0079 \pm 0.0019 \mu M$) (*SI Appendix*, Fig. S2). It inhibits FB with an IC$_{50}$ value of $0.01 \pm 0.006 \mu M$ ($n = 6$) (*SI Appendix*, Fig. S3*A*) and demonstrated potent inhibition of AP-induced MAC formation in 50% human serum (IC$_{50}$ value of $0.13 \pm 0.06 \mu M$) (*SI Appendix*, Table S3). In addition, the inhibitor is highly selective for FB, showing no inhibition of FD, no inhibition of classical or lectin complement pathway activation (up to 100 μM), and no significant effects (up to 10 μM) in a broad assay panel of receptors, ion channels, kinases, and proteases (*SI Appendix*, Table S3).

To evaluate the inhibitory potential of LNP023 under physiologically relevant conditions, we assessed its effect on AP-mediated complement activation in 50% human whole blood. Intriguingly, the compound blocks zymosan-induced MAC formation with an IC$_{50}$ value of $0.15 \pm 0.02 \mu M$ ($n = 18$) (*SI Appendix*, Fig. S3*B*), a concentration that is significantly below that of endogenous FB in these samples (about 1–2 μM). Moreover, we generally find a good correlation between the IC$_{50}$ values for
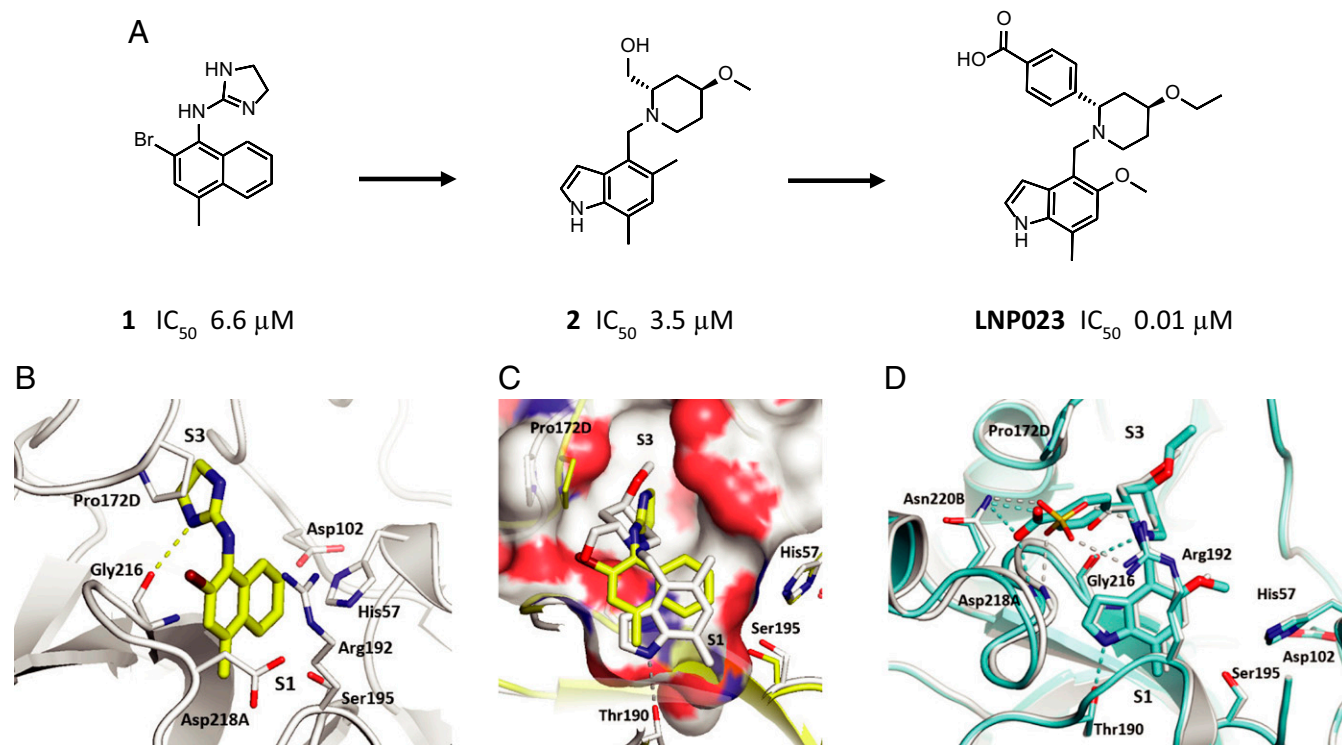

1 IC$_{50}$ 6.6 μM   **2** IC$_{50}$ 3.5 μM   **LNP023** IC$_{50}$ 0.01 μM

Fig. 1. Identification and structure-based optimization of a potent and selective FB inhibitor. (*A*) Chemical structure of compound **1**, compound **2**, and LNP023 and corresponding IC$_{50}$ values for inhibition of FB. (*B*) Cocrystal structure of human FB in complex with compound **1** (yellow sticks) at 1.64 Å resolution. (*C*) Overlay of compound **1** (yellow sticks) and compound **2** (white sticks) with close-up view into the S1 pocket. (*D*) Overlay of compound **2** (white sticks) and LNP023 (cyan sticks). A sulfate ion (yellow) from the cocrystal structure of compound **2** is shown. The catalytic residues His57 and Ser195 and other key residues of the ligand binding pockets are highlighted and shown as sticks.

FB inhibition and those for inhibition of MAC formation for a large number of inhibitors that we have generated during compound optimization, and as seen for LNP023, this correlation extends to compounds with IC$_{50}$ values considerably below the concentration of endogenous FB in the respective serum samples (*SI Appendix*, Fig. S4). Therefore, despite the similarity of the active sites of latent and convertase-associated FB (13), it appears that the compounds discriminate between the different FB forms and preferentially bind to the C3 and/or C5 convertase complex, or that the concentration of FB active sites is significantly lower than the total FB concentration. Alternatively, partial FB inhibition may be sufficient to stop the C3 amplification loop. In either case, latent FB does not appear to act as a scavenging sink for these inhibitors, suggesting that they should work in vivo at plasma exposures typical for small-molecule drugs.

We next studied the in vivo pharmacology of LNP023. The compound also strongly inhibits murine FB and blocks AP activation in 50% mouse serum with similar potency as in 50% human serum (*SI Appendix*, Table S3). i.p. injection of LPS induced a time-dependent increase in AP activation in the plasma of C57BL/6J mice as determined by rising levels of the C3 cleavage products C3d/iC3b (*SI Appendix*, Fig. S5A), and LNP023 effectively blocked complement activation when dosed orally at 30 mg/kg 3.5 h after LPS administration (*SI Appendix*, Fig. S5B). Moreover, the compound caused full plasma inhibition of AP activation over 8 h (*SI Appendix*, Fig. S5C) consistent with its pharmacokinetic profile (*SI Appendix*, Table S4) and indicating that inhibition of the AP in vitro can be fully recapitulated in vivo.

FB-deficient mice are protected from KRN/I-A^{g7} serum transfer-induced arthritis (19), suggesting a central pathogenic role of the AP in this model. We tested LNP023 in KRN-induced arthritis at doses of 20, 60, and 180 mg/kg twice a day (b.i.d.) and found the compound to be highly efficacious in reducing the overall clinical score (Fig. 2A). Full disease protection was seen at 60 and 180 mg/kg. In addition, LNP023, at all doses, significantly inhibited complement activation in the joints as evidenced by the strongly reduced levels of Ba, C3d, and C5a (Fig. 2B). Joint histological analysis showed that the inhibitor strongly blocked inflammatory cell infiltration (cellularity), bone erosion, and proteoglycan loss in all treated animals (Fig. 2C). These results indicate that LNP023 is able to prevent AP-mediated disease pathology to the same degree as FB-deficient mice (19) and to fully block complement activation in the relevant disease tissue.

Primary membranous nephropathy is frequently associated with nephrotic syndrome and can lead to end stage renal disease (20). It is typically caused by IgG4 autoantibodies to the M-type phospholipase A2 receptor on kidney podocytes resulting in subepithelial Ig deposits, activation of complement, and subsequent glomerular basement membrane injury. Activation of complement can be either lectin and/or alternative pathway mediated, and it has recently been found that FB-deficient mice do not develop proteinuria when immunized with the NC1 domain of human α3(IV) collagen as a model of membranous nephropathy (21). We show in a rat experimental model of membranous nephropathy that blocking the AP with LNP023 strongly ameliorated disease as demonstrated by the significant reduction in proteinuria, which was determined by the urinary total protein to creatinine ratio (Fig. 3A). Nephropathy in this model is induced by injection of an antiserum raised in sheep against a tubular epithelial fraction (Fx1A) from rat renal cortex (22), and LNP023 inhibits the AP in 50% rat serum with an IC$_{50}$ value of 0.56 ± 0.23 μM ($n = 12$). When given prophylactically starting at the time of disease induction, compound doses of 20 and 60 mg/kg had a similar efficacy in preventing proteinuria. Importantly, therapeutic dosing of LNP023 after onset of proteinuria (day 6) immediately halted further disease progression. Histologic analysis at the end of the study revealed the compound to significantly improve the overall histopathology score, greatly attenuate glomerulopathy (characterized
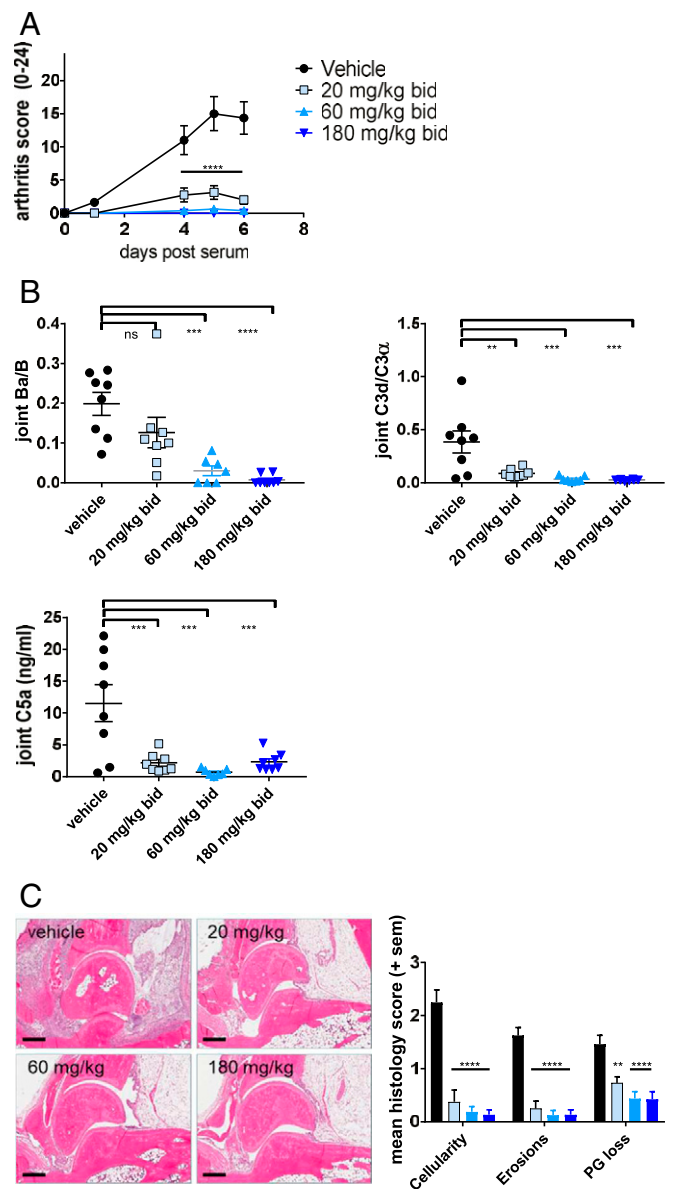

Fig. 2. LNP023 blocks KRN-induced arthritis. Arthritis was induced by KRN/I-Ag7 serum transfer in C57BL/6 mice 1 h after the first dose of compound ($n = 8$ mice per dose group). (A) Disease score was measured by joint swelling and shown as mean ± SEM. (B) Levels of complement activation products Ba, C3d, and C5a in the joint. (C) Representative images of joint histological analysis (H&E stain) and evaluation of inflammatory cell infiltration, bone erosion, and proteoglycan (PG) loss (safranin O staining) after 6 d of treatment. Vehicle (black bars), 20 mg/kg b.i.d. (light blue bars), 60 mg/kg b.i.d. (medium blue bars), and 180 mg/kg b.i.d. (dark blue bars). Data are mean ± SEM. P values were calculated using one-way ANOVA followed by Dunnett's multiple comparison test with a single pooled variance (for complement activation fragments and histology) or repeat measure two-way ANOVA followed by Dunnett's multiple comparison test; **$P < 0.01$, ***$P < 0.001$, ****$P < 0.0001$. (Scale bars, 400 μm.)

by enlarged glomeruli, basal membrane and Bowman's capsule thickening, and enlarged/rounded podocytes) (Fig. 3B), and prevent tubular degeneration (Fig. 3C) upon both prophylactic and therapeutic dosing. In addition, near-complete inhibition of complement activation, as judged by the absence of glomerular C3 deposition in most animals, was seen after compound treatment (Fig. 3D). Therefore, LNP023 is able to block AP activity in the kidney and stop glomerular disease progression in an
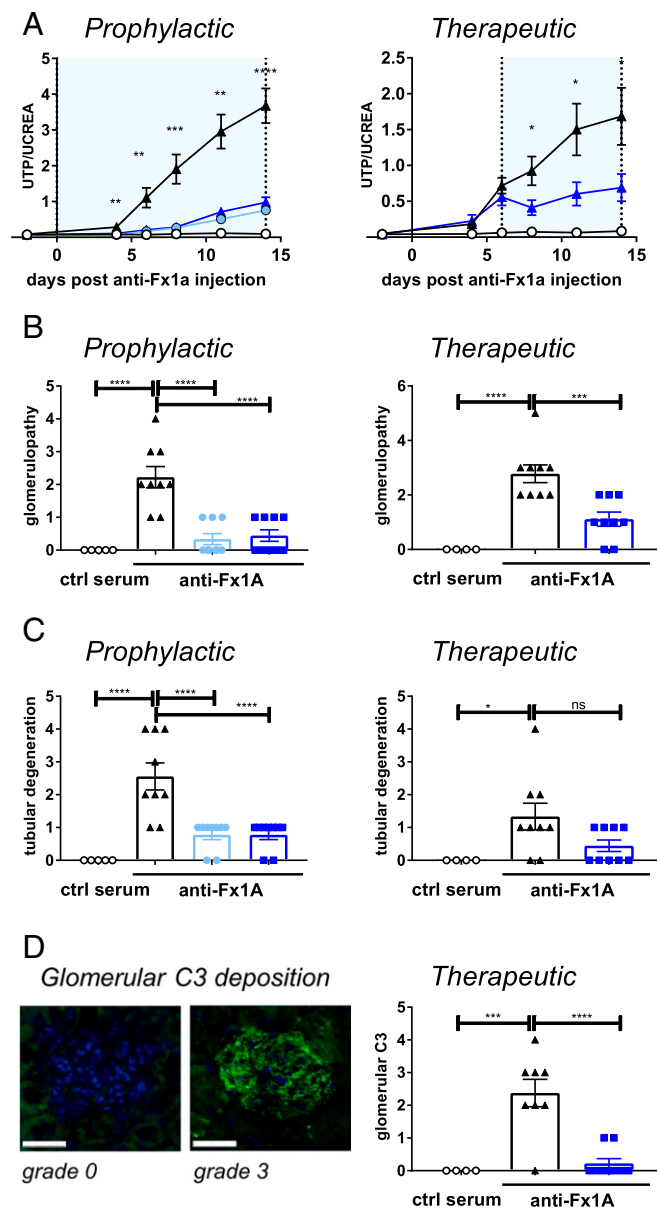
Fig. 3. Efficacy of LNP023 in an experimental model of membranous nephropathy. Passive Heymann nephritis was induced by injection of an anti-fraction 1A (anti-Fx1A) antibody serum, and LNP023 was dosed either prophylactically starting at day 0 or therapeutically starting at day 6 after disease onset. Nine animals were used per treatment group, and five animals received control (ctrl) serum. Light blue bars/symbols, 20 mg/kg b.i.d.; dark blue bars/symbols, 60 mg/kg b.i.d. (*A*) Proteinuria as determined by the urinary ratio of total protein (UTP) and creatinine (UCREA). The light blue areas indicate the duration of compound dosing. Open circles, control serum; black triangles, vehicle; blue filled circles, LNP023 20 mg/kg; blue triangles, LNP023 60 mg/kg. (*B*) Glomerulopathy (as characterized by enlarged glomeruli, basal membrane and Bowman's capsule thickening, and enlarged/rounded podocytes) and (*C*) tubular degeneration were determined by histopathological analysis after H&E staining on day 14 (therapeutic dosing) or day 15 (prophylactic dosing). (*D*) Glomerular C3 deposition. (*Left*) Representative histological staining of glomerular C3 deposition (grade 0 and 3). (Scale bars, 50 μm.) (*Right*) Glomerular C3 deposition after therapeutic dosing of LNP023 (day 15). Data are mean ± SEM. *P* values were calculated using one-way ANOVA followed by Dunnett's multiple comparison test with a single pooled variance (for complement activation fragments and histology) or repeat measure two-way ANOVA followed by Dunnett' multiple comparison test; *$P < 0.05$, **$P < 0.01$, ***$P < 0.001$, ****$P < 0.0001$.

autoantibody-driven animal model suggesting its potential therapeutic value for the treatment of human membranous nephropathy.

C3 convertase activity is highly up-regulated in the serum of C3G patients (6). The disease is caused by C3 convertase dysregulation due to the presence of C3 convertase stabilizing autoantibodies (C3 nephritic factors) and/or mutations in complement proteins leading to glomerular deposition of C3 cleavage products and chronic kidney disease. Addition of LNP023 to C3G patient sera blocked abnormal C3 cleavage (Fig. 4*A*). However, a higher compound concentration (>3 μM) was needed for full inhibition of C3 convertase activity than for inhibition of MAC formation in healthy serum (IC$_{50}$ value of 0.12 μM; *SI Appendix*, Table S3). This difference likely reflects the high level of AP activity in patient sera. C3 cleavage in this assay is, to some extent, dependent on newly formed C3 convertase since an FD inhibitor (23) (*SI Appendix*, Fig. S6) is also efficacious, albeit requiring high FD inhibitor exposures. We next tested the FB and FD inhibitors for their ability to prevent C3G serum-induced hemolysis of sheep erythrocytes, a measure of surface-bound complement activation. In the presence of EGTA, hemolysis is dependent on a hyperactivated AP provided by the patient samples (hemolysis is driven by the formation of C3 convertase on the erythrocyte surface). Both compounds potently blocked hemolysis at 0.15 μM (Fig. 4*B*). However, since inhibition of fluid phase AP activity in C3G is more readily achieved by targeting FB than FD (cf. Fig. 4*A*), it appears that steady state AP activity in C3G serum is more strongly driven by C3 convertase stabilization than by its production. In line with this hypothesis, the FB inhibitor was able to block hemolysis of C3 convertase-coated sheep erythrocytes in the presence of C3G patient-derived C3 nephritic factors, which was not the case for the FD inhibitor (Fig. 4*C*). These data suggest that blocking the AP at the level of the C3 convertase with a FB inhibitor might have an advantage over FD inhibition for the treatment of C3G patients.

Finally, we tested LNP023 for its ability to prevent the lysis of PNH erythrocytes. The disease is induced by a somatic mutation in the PIG-A gene in hematopoietic stem cells resulting in a deficiency of GPI-anchored proteins, including complement regulators CD55 and CD59, and leading to episodic complement-mediated hemolysis (24). Using erythrocytes from PNH patients, we found that LNP023 is able to block C3 deposition on the surface of CD59-negative erythrocytes (Fig. 4*D* and *SI Appendix*, Fig. S7) and prevent their lysis with an IC$_{50}$ value of 0.4 μM (Fig. 4*E*). While LNP023 was as effective as an FD inhibitor (23) and showed full inhibition in this assay, we confirmed previous findings that treatment with a neutralizing anti-C5 antibody is not able to fully block hemolysis in vitro (25). This is also seen in anti-C5–treated patients in vivo, even at saturating antibody concentrations (26). AP inhibition, therefore, potentially offers an advantage over the current standard of care anti-C5 therapy (27) by blocking not only intravascular hemolysis but also any C3-driven pathogenic event (28). Moreover, the development of FB inhibitors could lead to a therapy, which, by preventing C3-mediated intravascular and extravascular hemolysis, may improve hematological responses of PNH patients, possibly resulting in complete resolution of anemia and independence of blood transfusions (29).

Our results demonstrate that the AP can be efficiently blocked in vitro and in vivo at the level of the C3 convertase. LNP023 is a small-molecule FB inhibitor. The compound is highly selective and potent and is currently in clinical development for a number of complement-mediated diseases for which there are no satisfactory treatments available today, including C3G, PNH, IgA nephropathy, and membranous nephropathy.

Materials and Methods

Compound Synthesis and in Vitro Inhibition Assays. Details of compound synthesis are provided in *SI Appendix*. Compounds were tested for FB inhibition either by using CVF:Bb as stable surrogate of the C3 convertase and
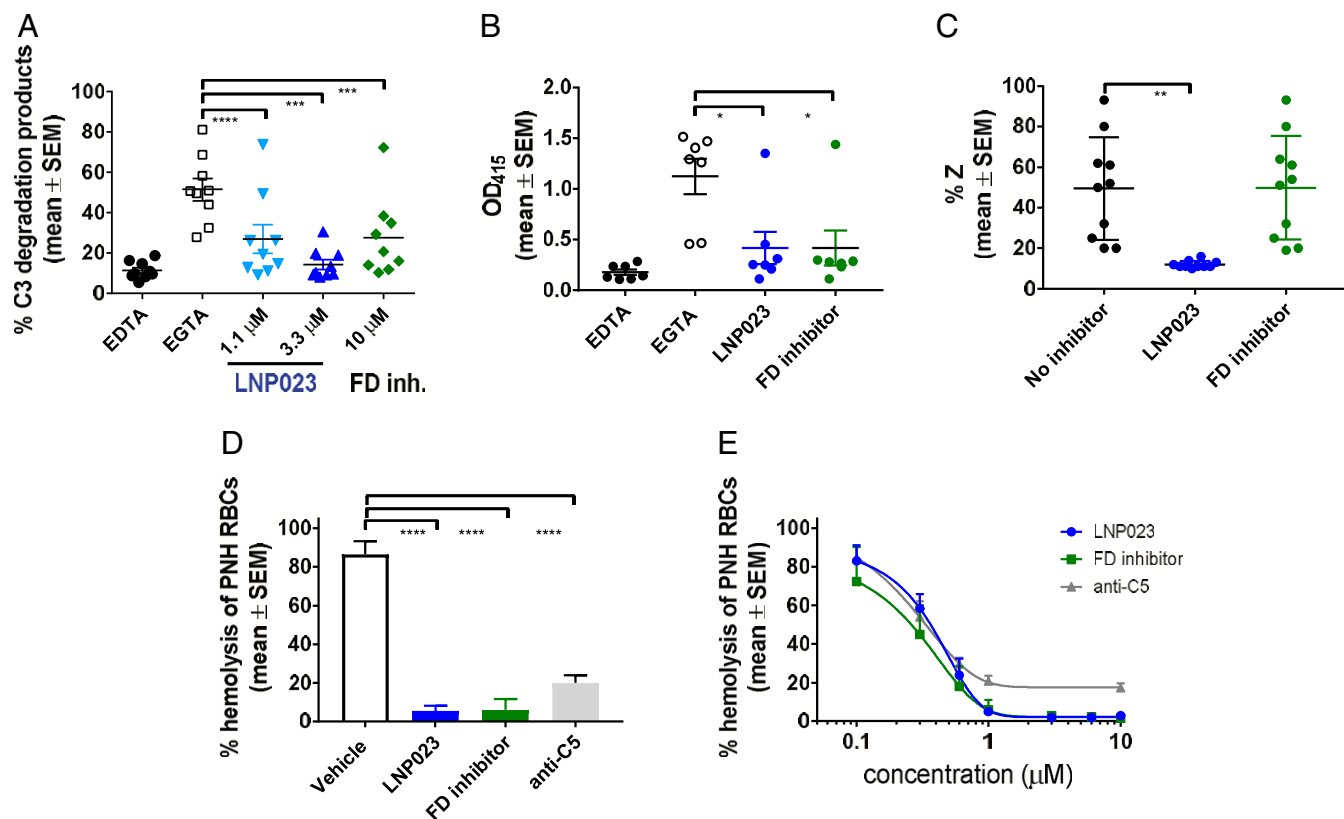
Fig. 4. LNP023 blocks complement activity in the serum of C3G patients and prevents lysis of human PNH erythrocytes. (*A*) Inhibition of C3 convertase activity in serum of C3G patients. Patient serum was incubated with normal human serum, and C3 degradation was detected by immunofixation electrophoresis and quantified. The AP is blocked in the presence of EDTA (maximum inhibition control) but not in the presence of Mg^{2+}-EGTA, which blocks the classical and lectin pathways. LNP023 is shown in light blue at 1.1 μM and dark blue at 3.3 μM, and an FD inhibitor is shown in green. (*B*) Prevention of C3G patient serum-induced hemolysis of sheep erythrocytes. Erythrocytes were incubated with C3G patient serum and LNP023 (0.15 μM) or an FD inhibitor (0.15 μM). Hemolysis was measured by increase in optical density at 415 nm. Addition of EDTA and EGTA was used as negative and positive control, respectively. (*C*) Inhibition of nephritic factor-stabilized C3 convertase activity. Sheep erythrocytes coated with preformed C3 convertase were incubated with total IgGs from C3G patient sera in the absence or presence of LNP023 (0.15 μM) or an FD inhibitor (0.15 μM). C3 convertase stabilized at 15 min was calculated as % Z ($Z_{15min}/Z_{0min} \times 100$). The assay was adjusted to yield one active C3 convertase per sheep erythrocyte ($Z_{0min} = 1$; *SI Appendix*). (*D*) Inhibition of hemolysis of PNH erythrocytes. Blood from three patients was analyzed in 2–14 repeats, mean ± SEM. Inhibitors were used at 1 μM. Hemolysis of PNH erythrocytes was determined by FACS analysis. (*E*) Dose–response curves for inhibition of hemolysis of erythrocytes from PNH patients for LNP023, FD inhibitor, and anti-C5 antibody. Hemolysis was measured by FACS analysis. Curves are representatives of three patients measured in 2–14 repeats. For each curve, the average per person from all repeats was used. *P* values were calculated using one-way ANOVA followed by Dunnett's multiple comparison test with a single pooled variance; *$P < 0.05$, **$P < 0.01$, ***$P < 0.001$, ****$P < 0.0001$.

purified endogenous C3 as substrate or by using a competition binding assay with FB and a Cy5-labeled small-molecule inhibitor as probe. AP inhibition was measured in 50% human serum or 50% human whole blood by following zymosan A-induced MAC formation. Serum or whole blood was preincubated with compound for 30 min before transfer to zymosan A-coated plates. MAC formation was detected with an anti-C9 neoepitope antibody by ELISA. AP complement deposition in mouse serum was measured in an analogous way except that C3b deposition was detected instead of MAC formation. Further details on protein purification and all in vitro assays are given in *SI Appendix*.

Protein Crystallography. Cocrystallization screening experiments were conducted with all compounds by using the catalytic domain (Asp470-Leu764) of human FB at a concentration of 25 mg/mL in 20 mM Tris, pH 7.5, containing 100 mM sodium chloride and 100 μM $ZnCl_2$. Crystals were grown at 20 °C using a sitting drop vapor diffusion format. Details of the crystallization conditions for all compounds are given in *SI Appendix*. All crystals were cryocooled in liquid nitrogen without the addition of cryoprotectant, and data were collected at the PXII beamline of the Swiss Light Source (SLS) at the Paul Scherrer Institut (PSI). Data collection and refinement statistics are shown in *SI Appendix*, Table S2. Crystal structures were solved by molecular replacement using the published structure of the catalytic domain (Protein Data Bank 1DLE). Structures were built and refined using Coot (30) and Refmac (31).

In Vivo Studies. Animal studies were performed in accordance with the Basel Cantonal Veterinary Committee. Animals were orally gavaged with vehicle [0.5% (wt/vol) methyl cellulose (MC), 0.5% (vol/vol) Tween 80] or LNP023 compound formulation (in vehicle) at the indicated doses. For KRN arthritis, disease was induced by tail vein i.v. injection of 150 μL K/BxN serum 1 h after compound or vehicle dosing. Swelling of hind paws was scored on a composite scoring scale of 0–24 per mouse. Front paws were snap frozen for subsequent lysate preparation for further analyses, hind paws were taken for histopathological processing, and serum was taken for ELISA and Western blotting.

Passive Heymann nephritis was induced by tail vein i.v. injection of sheep anti-rat Fx1A serum (5 mL/kg) into 7-wk-old male Sprague–Dawley rats. Compound or vehicle dosing was initiated 1 h before induction with Fx1A serum or on day 6 and continued b.i.d. until the end of the experiment on day 14. Urine was collected for the determination of creatinin, albumin, and total protein. At day 14 (therapeutic study) or day 15 (prophylactic study) after anti-Fx1A injection, a necropsy was performed, and kidneys were collected and processed for histopathology. Further details on all animal studies are provided in *SI Appendix*.

Ex Vivo Studies with Patient Samples. All studies were conducted in accordance with the Declaration of Helsinki and approved by the respective institutional and/or licensing committees (Ethikkommission Nordwest- und Zentralschweiz for use of human blood under the Novartis Basel tissue donor program; Human Subjects Office/Institutional Review Board, University of Iowa, for C3G samples; and Comitato Etico Università Federico II for PNH samples), and all patients gave informed consent before donating samples.

For inhibition of complement activity in C3G patient serum, C3 cleavage products were detected by immunofixation electrophoresis as previously described (32) and further detailed in *SI Appendix*. C3G patient serum-induced hemolysis of nonsensitized sheep erythrocytes was tested in 20% patient serum in the presence of compound or vehicle at 37 °C for 30 min, and hemolysis was quantified by measuring the optical density in the supernatant at 415 nm. To test whether LNP023 inhibits active C3 convertase stabilized with C3 nephritic factors (C3Nefs), the C3 complement stabilization assay was performed with sheep erythrocytes as previously described (32) (further details in *SI Appendix*). To perform the assay, 500 μg of patient IgG (containing C3Nefs) in 220 μL of EDTA-GVB buffer was mixed with 30 μL of C3 convertase-coated sheep erythrocytes (1×10^9/mL). C3 convertase was allowed to decay at 30 °C for 0, 7.5, 15, and 22.5 min, and at each time point, 50 μL was transferred to an empty 96-well plate, and hemolysis was induced by the addition of 50 μL of rat EDTA serum in the absence or presence of LNP023 or an FD inhibitor at the indicated concentration.

Ex vivo hemolysis and C3-opsonization of PNH erythrocytes was measured by flow cytometry. Erythrocytes from PNH patients were obtained from peripheral blood after three washings in saline and were subsequently incubated with Mg^{2+}-supplemented sera from ABO-matched healthy individuals [normal human serum (NHS)] at final hematocrits of 2%. To reduce interexperiment variability, pooled sera from at least three subjects all with plasma C3 levels in the normal range (0.9–1.8 g/L) were used. AP activation was achieved by acidification using HCl (1:20 of 0.1 M HCl), which resulted in a drop in the pH value to between 6.7 and 6.9. Compound was added to the tubes at different concentrations before complement activation. After 24 h incubation time at 37 °C in acidified NHS, hemolysis was quantified after staining of the erythrocyte pellet with a FITC-conjugated anti-C3 polyclonal antibody and a PE-conjugated anti-CD59 monoclonal antibody. The same anti-C3 and anti-CD59 staining also served to assess opsonization. Further details are provided in *SI Appendix*.

Data Availability. Atomic coordinates and structure factors for human FB in complex with compounds **1**, **2**, and LNP023 have been deposited in the Protein Data Bank (accession nos. 6QSW, 6QSX, and 6QSV, respectively). All data are available in the main text or *SI Appendix*.

1. Walport MJ (2001) Complement. First of two parts. *N Engl J Med* 344:1058–1066.
2. Ricklin D, Hajishengallis G, Yang K, Lambris JD (2010) Complement: A key system for immune surveillance and homeostasis. *Nat Immunol* 11:785–797.
3. Schramm EC, et al. (2014) Genetic variants in the complement system predisposing to age-related macular degeneration: A review. *Mol Immunol* 61:118–125.
4. Brodsky RA (2014) Paroxysmal nocturnal hemoglobinuria. *Blood* 124:2804–2811.
5. Rodríguez de Córdoba S, Hidalgo MS, Pinto S, Tortajada A (2014) Genetics of atypical hemolytic uremic syndrome (aHUS). *Semin Thromb Hemost* 40:422–430.
6. Barbour TD, Pickering MC, Cook HT (2013) Recent insights into C3 glomerulopathy. *Nephrol Dial Transplant* 28:1685–1693.
7. Łukawska E, Polcyn-Adamczak M, Niemir ZI (2018) The role of the alternative pathway of complement activation in glomerular diseases. *Clin Exp Med* 18:297–318.
8. Oppermann M, et al. (1991) Elevated plasma levels of the immunosuppressive complement fragment Ba in renal failure. *Kidney Int* 40:939–947.
9. Reynolds R, et al. (2009) Plasma complement components and activation fragments: Associations with age-related macular degeneration genotypes and phenotypes. *Invest Ophthalmol Vis Sci* 50:5818–5827.
10. Silva AS, et al. (2012) Plasma levels of complement proteins from the alternative pathway in patients with age-related macular degeneration are independent of complement factor H Tyr[402]His polymorphism. *Mol Vis* 18:2288–2299.
11. Lachmann PJ, Hughes-Jones NC (1984) Initiation of complement activation. *Springer Semin Immunopathol* 7:143–162.
12. Milder FJ, et al. (2007) Factor B structure provides insights into activation of the central protease of the complement system. *Nat Struct Mol Biol* 14:224–228.
13. Forneris F, et al. (2010) Structures of C3b in complex with factors B and D give insight into complement convertase formation. *Science* 330:1816–1820.
14. Rooijakkers SH, et al. (2009) Structural and functional implications of the alternative complement pathway C3 convertase stabilized by a staphylococcal inhibitor. *Nat Immunol* 10:721–727.
15. Ponnuraj K, et al. (2004) Structural analysis of engineered Bb fragment of complement factor B: Insights into the activation mechanism of the alternative pathway C3-convertase. *Mol Cell* 14:17–28.
16. Ruiz-Gómez G, et al. (2009) Structure-activity relationships for substrate-based inhibitors of human complement factor B. *J Med Chem* 52:6042–6052.
17. Smith CA, Vogel CW, Müller-Eberhard HJ (1982) Ultrastructure of cobra venom factor-dependent C3/C5 convertase and its zymogen, factor B of human complement. *J Biol Chem* 257:9879–9882.
18. Schechter I, Berger A (1967) On the size of the active site in proteases. I. Papain. *Biochem Biophys Res Commun* 27:157–162.
19. Ji H, et al. (2002) Arthritis critically dependent on innate immune system players. *Immunity* 16:157–168.
20. Couser WG (2017) Primary membranous nephropathy. *Clin J Am Soc Nephrol* 12:983–997.
21. Luo W, et al. (2018) Alternative pathway is essential for glomerular complement activation and proteinuria in a mouse model of membranous nephropathy. *Front Immunol* 9:1433–1444.
22. Jefferson JA, Pippin JW, Shankland SJ (2010) Experimental models of membranous nephropathy. *Drug Discov Today Dis Models* 7:27–33.
23. Maibaum J, et al. (2016) Small-molecule factor D inhibitors targeting the alternative complement pathway. *Nat Chem Biol* 12:1105–1110.
24. Risitano AM (2013) Paroxysmal nocturnal hemoglobinuria and the complement system: Recent insights and novel anticomplement strategies. *Adv Exp Med Biol* 735:155–172.
25. Harder MJ, et al. (2017) Incomplete inhibition by eculizumab: Mechanistic evidence for residual C5 activity during strong complement activation. *Blood* 129:970–980.
26. Sica M, et al. (2017) Eculizumab treatment: Stochastic occurrence of C3 binding to individual PNH erythrocytes. *J Hematol Oncol* 10:126–136.
27. Loschi M, et al. (2016) Impact of eculizumab treatment on paroxysmal nocturnal hemoglobinuria: A treatment versus no-treatment study. *Am J Hematol* 91:366–370.
28. Risitano AM, et al. (2009) Complement fraction 3 binding on erythrocytes as additional mechanism of disease in paroxysmal nocturnal hemoglobinuria patients treated by eculizumab. *Blood* 113:4094–4100.
29. Risitano AM, Marotta S (2018) Toward complement inhibition 2.0: Next generation anticomplement agents for paroxysmal nocturnal hemoglobinuria. *Am J Hematol* 93:564–577.
30. Emsley P, Lohkamp B, Scott WG, Cowtan K (2010) Features and development of Coot. *Acta Crystallogr D Biol Crystallogr* 66:486–501.
31. Murshudov GN, Vagin AA, Dodson EJ (1997) Refinement of macromolecular structures by the maximum-likelihood method. *Acta Crystallogr D Biol Crystallogr* 53:240–255.
32. Zhang Y, et al. (2012) Causes of alternative pathway dysregulation in dense deposit disease. *Clin J Am Soc Nephrol* 7:265–274.

IMMUNOLOGY AND INFLAMMATION